

performed by Mrs. Karin Baum, Mrs. Ruth Childs, Miss Ana Maria Leoni, and Mrs. Sirpa Lessig. The experiment could not have been performed without their work. The endless checking and remeasuring of the film was greatly facilitated

through the dedication, and good humor, of Mr. John Neves.

Finally the authors wish to thank Mr. Peter Martin and the rest of the technical staff of this laboratory.

*Research supported by the U.S. Atomic Energy Commission under contract AT(11-1)3075.

†Present address: Physics Department, The Johns Hopkins University, Baltimore, Maryland 21218.

¹P. W. Lucas, H. D. Taft, and W. J. Willis, preceding paper, Phys. Rev. D **8**, 719 (1973).

²Terry S. Mast, Lawrence K. Gershwin, Margaret Alston-Garnjost, Roger O. Bangerter, Angela Barbaro-Galtieri, Joseph J. Murray, Frank T. Solmitz, and Robert D. Tripp,

Phys. Rev. **183**, 1200 (1969).

³N. P. Samios, Phys. Rev. **121**, 275 (1961).

⁴D. W. Joseph, Nuovo Cimento **16**, 997 (1960).

⁵Edward S. Ginsberg, Phys. Rev. **162**, 1570 (1967).

⁶D. Davison, R. Bacastow, W. H. Barkas, D. A. Evans, S.-Y. Fung, L. E. Porter, R. T. Poe, and D. Greiner, Phys. Rev. **180**, 1333 (1969).

⁷Particle Data Group, Rev. Mod. Phys. **43**, S1 (1971).

⁸P. Lucas, thesis, Yale University, 1972 (unpublished).

Study of $K^+p \rightarrow K^+p2\pi^+2\pi^-$ at 12.7 GeV/c

P. L. Jain, W. M. Labuda, Z. Ahmad, and G. Pappas

High Energy Experimental Laboratory, Department of Physics, State University of New York at Buffalo, Buffalo, New York 14214

(Received 16 March 1973)

We present the results of the reaction $K^+p \rightarrow K^+p2\pi^+2\pi^-$ at 12.7 GeV/c. These results are compared with the predictions of the model developed by Chan, Łoskiewicz, and Allison (the CŁA model) and with a modified form of this model. With the addition of resonance production to the model, adequate predictions of the experimental distributions are obtained. The data were also analyzed in terms of the quark model for hadronic structure which is revealed through the distributions of longitudinal momentum, transverse-momentum squared, and the rapidity for the negative pions.

I. INTRODUCTION

The study of many particle processes in high-energy collisions is in a very early stage of development. Owing to their intrinsic complexity, our understanding of these processes lags far behind that of two-body reactions, which are relatively simple compared to many-body reactions. In many-body reactions the dimensionality of phase space increases rapidly so that one needs too many variables to describe all features of a reaction. In recent years there has been a growing interest among both the experimentalists and theoreticians in the study of many-body reactions. The progress in understanding high-multiplicity reactions has mainly been made through a number of theoretical models, for example (i) the bremsstrahlung model,¹ (ii) the thermodynamic model,² (iii) the quark model,³ and (iv) the multi-Regge model.^{4,5} The last [(iv)] model, a version of the multiperipheral

model, has been extensively used to interpret the experimental data. A model of this type, aimed at describing inelastic reactions quantitatively, has been proposed by Chan, Łoskiewicz, and Allison⁶ (known as the CŁA model), and has been shown by various experimental groups⁷ to reproduce the main features of many body reactions.

In experiments in which pions are used as projectiles, the leading pion can be easily lost among the other pions produced. However, when the projectile is a kaon, the leading particle among the secondaries can be distinguished from the directly-produced pions on the basis of their mass difference. From the detailed analysis of multiple meson production in high-energy kaon-nucleon collisions in terms of a multi-Regge model, one can learn a great deal about the range of applicability and usefulness of the model. Hence, we present here the results for the reaction $K^+p \rightarrow K^+p2\pi^+2\pi^-$ at 12.7 GeV/c and compare them with the predic-

tions of the CLA model and a modified CLA model. We have also analyzed our data in the quark frame of reference³ and find that some of the predictions of the quark model, using simple dynamical assumptions about the quark-quark interaction amplitude, appear to be remarkably correct.

II. EXPERIMENTAL PROCEDURE

The data used in this experiment were obtained from the film exposed at the Brookhaven National Laboratory. The BNL 80-in. hydrogen bubble chamber was exposed to a 12.7-GeV/c K^+ beam from the AGS and ~150 000 pictures were taken. A sample of 10 980 pictures was scanned twice for all six-prong events. The over-all scanning efficiency for observing six-prong events was 98%. We recorded 1700 six-prong events which are analyzed here. The geometrical reconstruction and Kinematic fitting were done using the programs TVGP and SQUAW, respectively. Kinematic fits were obtained for the reactions $K^+p \rightarrow K^+p2\pi^+2\pi^-$ and $K^+p \rightarrow K^+p2\pi^+2\pi^- + \text{missing mass}$. In the attempts to fit to a particular reaction, each of the positively charged tracks was tested with the three mass hypotheses (pion, kaon, and proton). We also made use of the ionization of the tracks which must also be consistent with the calculated ionization value determined by the SQUAW fitting program. In Fig. 1 the plot of the square of the missing mass for events making four-constraint fits clearly shows a strong peaking near 0.0 GeV. The

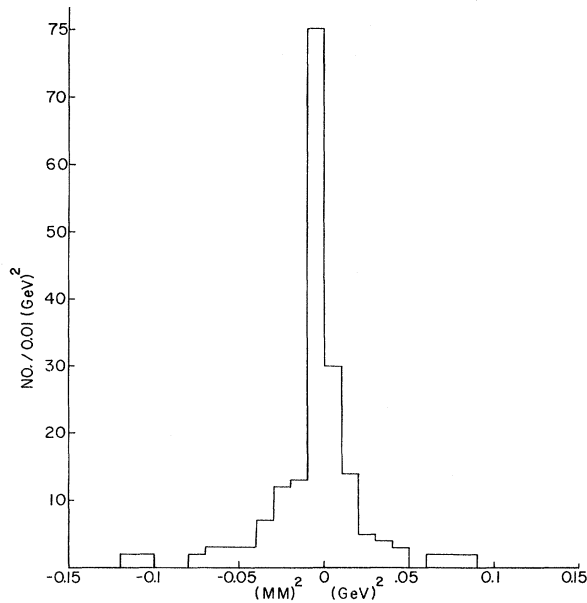


FIG. 1. Distribution of the square of the missing mass for events making 4-constraint fit for $K^+p \rightarrow K^+p2\pi^+2\pi^-$.

events were selected on the basis of the goodness of the fit ($\chi^2 < 20$).

III. THEORETICAL DISCUSSION

A. Multiperipheral Reggeized Model

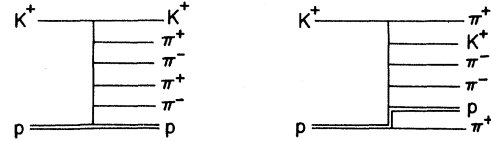
Previous experiments have shown that for incident momentum greater than ~3 GeV/c, the multiperipheral Regge model gives a rather good description of the production phenomena. Here we use the model of Chan *et al.*⁶ (CLA) in which the amplitude is modified to take into account the resonance production observed in our data. We assume that the reaction can be described by an incoherent sum of multiperipheral graphs, two of which are shown in Fig. 2(a). The others are obtained by the permutations of the outgoing particles consistent with known exchanges. The total amplitude for the reaction is given by

$$A \sim \prod_i^{n-1} A_i,$$

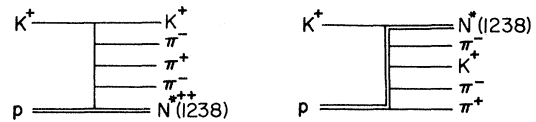
where A_i is the CLA amplitude for the i th exchange in the chain, i.e.,

$$A_i = \left(\frac{g_i s_i + ca}{s_i + a} \right) \left(\frac{s_i + a}{a_i} \right)^{\alpha_i} \left(\frac{s_i + b_i}{b_i} \right)^{\alpha_i' t_i},$$

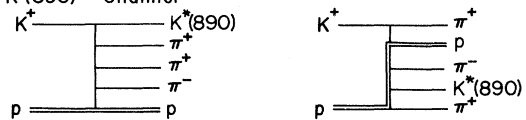
(a) Non-resonant Channel



(b) $N^*(1238)$ Channel



(c) $K^*(890)$ Channel



(d) $N^*(1238)$ and $K^*(890)$

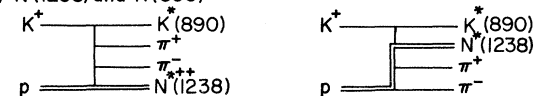


FIG. 2. Graphs used for CLA model calculations.

and

$$s_i = (p_i + p_{i+1})^2 - (m_i + m_{i+1})^2$$

and

$$t_i = \left(p_A - \sum_{r=1}^i p_r \right)^2,$$

where p_A is the four-momentum of the incident particle, the p_i 's are the four-momenta of the final-state particles, the s_i 's are the partial energies for each pair of particles, and the t_i 's are the squares of the four-momentum transfers between particles. α_i is the intercept of the i th Regge trajectory; α'_i is the slope of the exchanged trajectory; a is a constant that represents an energy scale which divides the low and high energy regions; b_i is a constant which describes the exponential dependence of the Regge couplings on t ; and c is the constant which describes the strength of the phase-space contribution when s_i is small. We made use of the values^{6,8} given in Table I. As there are a large number of possible diagrams, certain simplifying assumptions were made in applying the model. It was assumed that the experimental distribution could be reproduced if average trajectories and associated average coupling con-

TABLE I. Parameters used in CZA model.^a

Trajectory	α (intercept of trajectory)	g (relative coupling const.)
Nucleon	-0.35	1.4
Hyperon	-0.35	1.4
Kaon	0.30	1.0
Pomeranchukon	1.0	0.7
Meson	0.5	1.0

^a For b_i we take the values of 0.5 and 1.0 and 1.2 for the target proton vertex, incident K^+ vertex, and internal vertices, respectively. For a and c we used 1.0 and 1.4, respectively.

stants were used instead of exact values. This clearly reduced the number of possible diagrams significantly. Possible exchanges for K^+p interactions include nucleon-hyperon, kaon, Pomeranchukon, and meson. The various quantum numbers, average trajectories, and coupling constants used are listed in Table I.

Resonance effects have also been included in the model. Various diagrams are constructed as illustrated in Figs. 2(a), 2(b), 2(c), and 2(d). The reaction probability may then be expressed as

$$|A|^2 = f_0 \sum_{\text{nonres}} (A_i^0)^2 + f_1 \sum_{R_1} [A_i^1 F_{\text{BW}}(R_1)]^2 + f_2 \sum_{R_2} [A_i^2 F_{\text{BW}}(R_2)]^2 + \dots + f_K \sum_{R_K} [A_i^K F_{\text{BW}}(R_1) F_{\text{BW}}(R_2)]^2 + \dots, \quad (1)$$

where f_0, f_1, \dots are the experimentally determined fractions for each of the channels above. The R_j 's represent the resonant states present, and $F_{\text{BW}}(R_j)$, the Breit-Wigner form for a given resonance. The A_i^0 's and A_i^k 's are the nonresonant- and resonant-channel amplitudes, respectively. The model is applied by generating Monte Carlo events which are weighted according to the incoherent sum of amplitudes for all possible exchange diagrams.

The resonance production has been included only for the significantly produced resonances $N^{*+}(1238)$ and $K^*(890)$. The total number of diagrams for different channels (including those with resonances) is 90.

B. Modified Multiperipheral Model

It is found that the single-particle distributions are not quantitatively reproduced in every respect by the CZA model. This may be due to the assumption in the CZA model that the scattering amplitude may be parametrized by an exponential-like function of the four-momentum transfer squared. For many body final states, the four-momentum transfer squared ($-t$) distributions do

not exhibit exponential dependence.⁹ This is to a large extent due to the influence of kinematics and phase-space factors. Exponential dependence is obtained, however, for t' distributions, where $t' = |t - t_{\text{min}}|$, and t_{min} is the threshold value of the four-momentum transfer required to produce the given effective mass (M_A) for the system of particles ($K^+\pi^+\pi^-\pi^+\pi^-$). For the case of t'_{pp} we find

$$t_{\text{min}} = (E_p - E_{\text{min}})^2 - (p - p_{\text{min}})^2,$$

where

$$p_{\text{min}} = \{ [E_{\text{c.m.}}^2 + M_A^2 - m_p^2] / 2E_{\text{c.m.}} \}^2 - M_A^2 \}^{1/2},$$

and E_p is the energy of the incident proton in the c.m. system; m_p is the mass of the proton; $E_{\text{c.m.}}$ is the total energy in the c.m. system; E_{min} for the proton is given by $E_{\text{min}} = (p_{\text{min}}^2 + m_p^2)^{1/2}$. We have plotted the t'_{pp} distribution and found it to be exponential as shown in Fig. 3(b), while the t distribution in Fig. 3(a) is clearly not exponential. This change removes some of the kinematical effects which cause the four-momenta transfer to have a nonexponential-like distribution. Thus in the modified form of the CZA model, we have replaced the four-momentum transfer squared term t by t' .

IV. EXPERIMENTAL RESULTS

A. Single-Particle Distributions

1. Angular Distributions

Peripheralism is strongly indicated by the angular distributions of the outgoing proton and kaon. In Figs. 4(a) and 4(b) are shown the kaon and proton angular distributions in the c.m. system which show strong peaking in the forward and backward directions, respectively. For the study of pions as secondary produced particles from the pion-nucleon reaction, it is difficult to separate the projectile from the produced pions. However, in the reaction studied here the projectile is a kaon, and the leading particle can be easily separated from the produced pions on the basis of their mass difference.

The CZA model qualitatively reproduces the angular distributions of the proton and K^+ , but predicts the scattering angles to be somewhat smaller than those observed. This is particularly apparent for the positive kaon where the disagreement is relatively large. The modified CZA mod-

el, on the other hand, gives a more reasonable fit to the K^+ distribution. In Fig. 5 are shown the angular distributions for the π^+ and π^- pions exhibiting both forward and backward peaking in the c.m. system. A major cause for this peaking is the the abundant resonance production (~50% of the events). Here the peripherally produced resonant states decay and the decay products peak strongly in the forward and the backward directions. Theoretical fits with the CZA model as well as with modified CZA models were found to be excellent. The analysis of particle angular distributions is greatly affected by the presence of the common resonances, i.e., $N^{*++}(1238)$ and $K^{*0}(890)$. These resonances are found in the invariant-mass distributions of the proton and one of the positive pions for $N^{*++}(1238)$, and for positive kaon and one of the negative pions for $K^{*0}(890)$ in the region

$$\begin{aligned} 1.20 &\leq M(p\pi^+) \leq 1.30 \text{ GeV}, \\ 0.84 &\leq M(K^+\pi^-) \leq 0.94 \text{ GeV}. \end{aligned} \quad (2)$$

When these resonances are removed, the forward and backward peaks in the pion distribution dis-

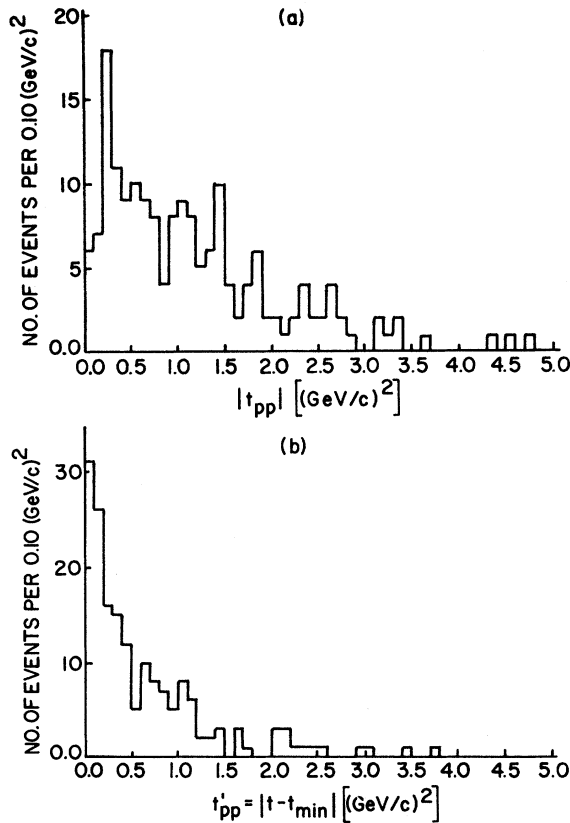


FIG. 3. Four-momentum-transfer squared from incoming proton to outgoing proton. (a) t'_{pp} and (b) $t'_{pp} = |t - t_{\min}|$ where t_{\min} is explained in the text.

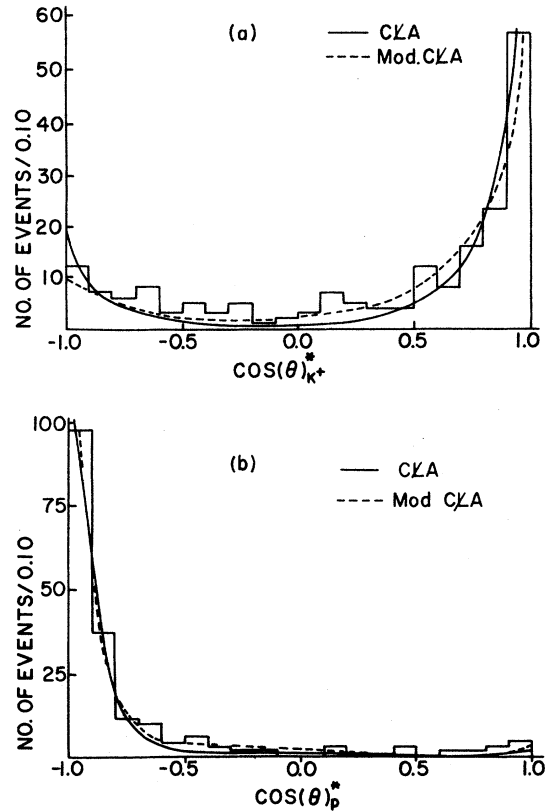


FIG. 4. The c.m. angular distributions of (a) kaons and (b) protons. The histograms display the experimental data and the smooth curves the theoretical predictions: (—) CZA and (---) modified CZA.

TABLE II. Asymmetry parameters [$A = (F - B)/(F + B)$] for p, K^+, π^+ , and π^- .

Asymmetry parameter	Value	Events removed with $1120 \leq M(p\pi^+) \leq 1360$ MeV	Events removed with $840 \leq M(K^+\pi^-) \leq 950$ MeV
A_p (proton)	-0.79 ± 0.04	-0.35 ± 0.08	-0.82 ± 0.06
A_{K^+} (K^+)	0.45 ± 0.06	0.20 ± 0.09	0.34 ± 0.09
A_{π^+} (π^+)	0.08 ± 0.04	0.46 ± 0.07	0.01 ± 0.06
A_{π^-} (π^-)	0.18 ± 0.05	0.21 ± 0.07	-0.05 ± 0.08

appear. This result is in agreement with data from other high multiplicity reactions.¹⁰

In Table II is shown the asymmetry ratio $A = (F - B)/(F + B)$ for the final-state protons, kaons, and pions, where F and B are the numbers of forward and backward events, respectively, in the c.m. system. For the proton and pion we observe a strong peripheralism. When we remove the resonance events we get a more symmetric sample. This is in agreement with data from other high multiplicities, where it is observed that resonance channels tend to produce a more peripheral interaction.

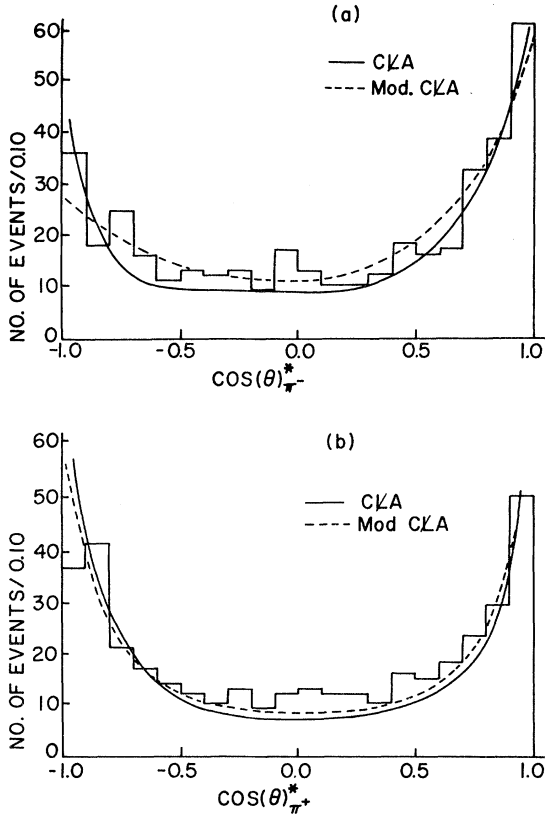


FIG. 5. The c.m. angular distributions of (a) π^- and (b) π^+ . The histograms display the experimental data and the smooth curves the theoretical predictions: (—) CZA and (---) modified CZA.

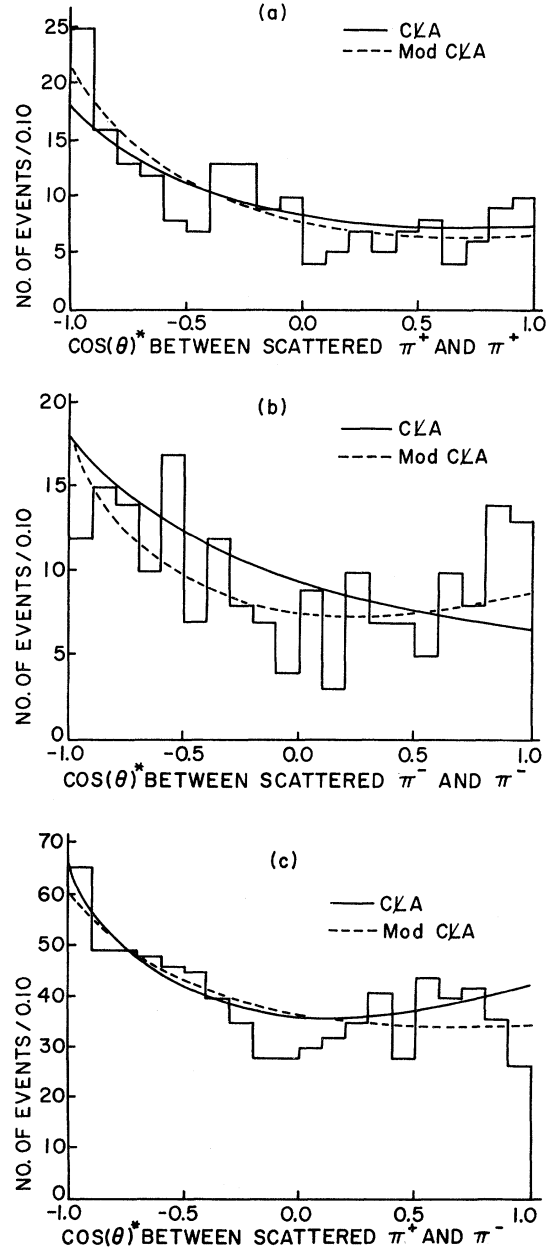


FIG. 6. Angular distribution in c.m. system between (a) two positive pions, (b) two negative pions, (c) positive and negative pions. (—) predictions of the CZA model; (---) predictions of the modified CZA model.

TABLE III. Values of the γ parameter for different pairs of particles in the reaction $K^+p \rightarrow K^+p2\pi^+2\pi^-$ in the c.m. system.

$\gamma = N_A/N_B$	Resonance not removed	Resonance N^{*++} removed	Resonance K^{*0} removed	Resonance N^{*++} and K^{*0} removed
$\gamma(\pi^+\pi^+)$	1.95 ± 0.42	1.62 ± 0.48	1.72 ± 0.42	1.19 ± 0.41
$\gamma(\pi^-\pi^-)$	1.23 ± 0.25	1.02 ± 0.29	1.23 ± 0.29	1.06 ± 0.36
$\gamma^L(\pi^+\pi^+)$	1.54 ± 0.23	1.28 ± 0.20	1.45 ± 0.25	1.12 ± 0.27
$\gamma^U(\pi^+\pi^-)$	1.22 ± 0.12	1.10 ± 0.16	1.19 ± 0.14	1.00 ± 0.17
$\gamma(K^+\pi^-)$	1.19 ± 0.14	0.99 ± 0.23	1.09 ± 0.36	1.02 ± 0.22
$\gamma(K^+\pi^+)$	1.47 ± 0.22	1.20 ± 0.28	1.43 ± 0.33	1.60 ± 0.39
$\gamma(P\pi^+)$	1.17 ± 0.17	3.53 ± 0.99	1.19 ± 0.27	2.09 ± 0.53
$\gamma(P\pi^-)$	1.92 ± 0.29	1.95 ± 0.51	1.51 ± 0.35	2.23 ± 0.57

2. Angular Correlation Between Pions [GGLP (Goldhaber-Goldhaber-Lee-Pais) Effect]

Goldhaber *et al.*¹¹ observed a significant difference in the distribution of the c.m. system angle between the pairs of pions of the like and unlike charges in $p\bar{p}$ annihilation at 1.05 GeV/c. Since that time similar differences have been observed at various momenta of the incoming \bar{p} and for different pion multiplicities in the final state. Similar effects have been observed in π^+p interactions at 4 GeV/c,¹² 5 GeV/c,¹³ and 8 GeV/c (see Ref. 14); in π^-p interactions at 11 GeV/c,¹⁵ and 16 GeV/c (see Ref. 16); in pp interactions at 10 GeV/c (see Ref. 17); and in K^+p interactions at 5 GeV/c.¹⁸ Goldhaber *et al.* observed that the average angle for pairs of unlike pions is greater than that for pairs of like pions and explained the GGLP effect as being due to the symmetrization of the pion wave function required by Bose-Einstein statistics. They proposed to investigate the energy dependence of the effect, and later it was found¹⁹ to be in strong disagreement with the predictions of Goldhaber *et al.*¹¹ The observed effect depends rather strongly on the details of the interaction mechanism. In the calculation of Goldhaber *et al.*,¹¹ resonance production was not taken into consideration, and it was observed¹⁹ that in low-multiplicity events the ρ meson strongly affects the observed difference of γ^{+-} and $\gamma^{\pm\pm}$ in $p\bar{p}$ annihilation, where γ is equal to the ratio of the number of pairs with opening angle greater than 90° to that with opening angle smaller than 90° in the c.m. system. For pairs of pions with like and unlike charges we write γ^{++} , γ^{--} , and γ^{+-} , respectively. It has been found that (i) $\gamma^{++} > \gamma^{--}$ for primary π^+ , and (ii) $\gamma^{--} > \gamma^{+-}$ for primary π^- . The effect has been attributed possibly to the "leading pion" which plays an important role when the incident energy increases.

To the best of our knowledge, the $\pi\pi$ angular correlation has not been observed with primary

K^+ mesons in its interaction with protons at energies greater than 8 GeV/c. We present here evidence for such a correlation in K^+p interactions at 12.7 GeV/c with six prongs, i.e., K^+p

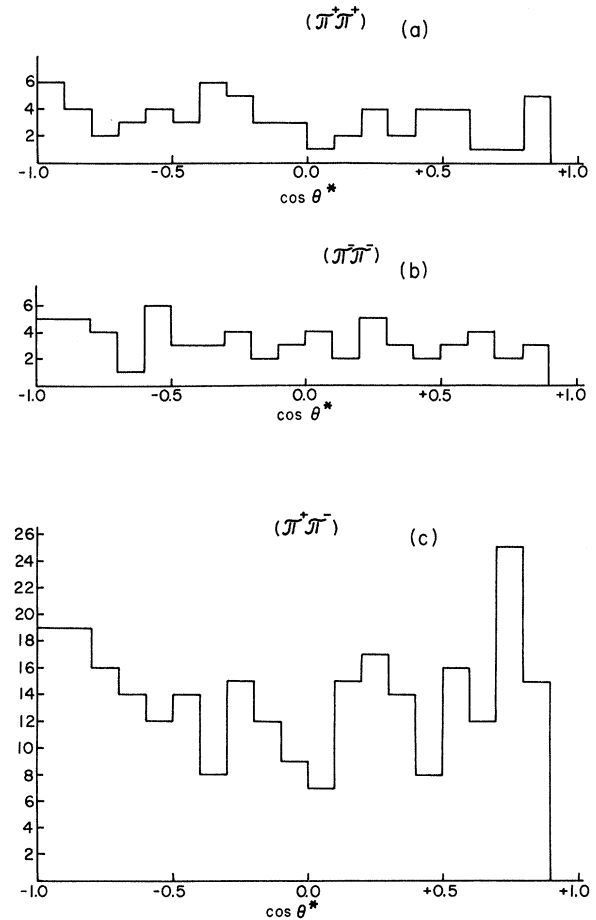


FIG. 7. Angular distributions in c.m. system between two pions after the removal of resonances. (a) Two positive pions; (b) two negative pions; (c) positive and negative pions.

$\rightarrow K^+p2\pi^+2\pi^-$. In Figs. 6(a), 6(b), and 6(c) are shown the distributions of the c.m. opening angle between the momenta of like ($\pi^+\pi^+$), ($\pi^-\pi^-$), and unlike ($\pi^+\pi^-$) pions, respectively, in the reaction $K^+p \rightarrow K^+p2\pi^+2\pi^-$. The theoretical curves are due to the predictions of the C \bar{L} A and modified C \bar{L} A models. The values of the parameter have been calculated for the pairs of the pions with like charges ($\pi^+\pi^+$, $\pi^-\pi^-$), i.e., γ^L is defined as $\gamma^L = N_A^L/N_B^L$ and for pairs of pions with unlike charges ($\pi^+\pi^-$), i.e., $\gamma^U = N_A^U/N_B^U$, where N_A and N_B are the numbers of pairs with an opening angle $\theta_{\pi\pi}$ greater than 90° and less than 90° , respectively. The values of γ are given in Table III. The distribution for like positive pions ($\pi^+\pi^+$) tends to be more peaked in the backward hemisphere. This feature is different from what has been observed in other multipion final states in antiproton-proton annihilations and in large-multiplicity pion-nucleon interactions.

In order to investigate the possible source of the effect, we study the peripheral production which is strongly indicated by the angular distribution of the outgoing kaon and proton. Figures 4(a) and

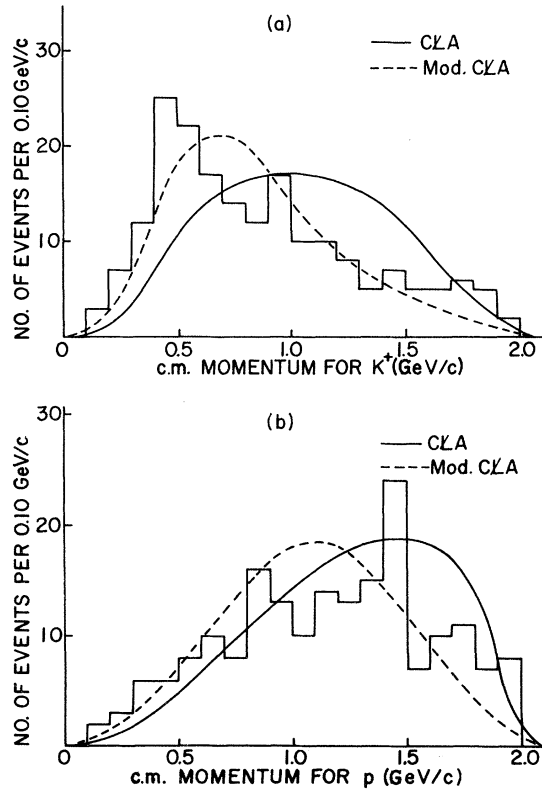


FIG. 8. The c.m. momentum distributions of (a) K^+ and (b) p . The histograms display the experimental data, and the smooth curves the theoretical predictions of (—) the C \bar{L} A model and (---) the modified C \bar{L} A model.

TABLE IV. Transverse and longitudinal momentum.

Particle	$\langle p_t \rangle$ (GeV/c)	$\langle p_t^* \rangle$ (GeV/c)	$\langle p_t^* \rangle$ (GeV/c)
p	0.46 ± 0.02	-0.86 ± 0.05	1.03 ± 0.05
K^+	0.44 ± 0.02	0.38 ± 0.05	0.68 ± 0.05
π^+	0.36 ± 0.01	0.04 ± 0.03	0.41 ± 0.03
π^-	0.35 ± 0.01	0.15 ± 0.03	0.39 ± 0.03

4(b) show that the distributions for kaon and proton are strongly peaked forward and backward, respectively. Figure 5 shows the angular distribution for the pions, exhibiting peaking in the c.m. system. It was pointed out earlier that the major cause of this peaking is the abundant resonance production (~50% of the events). In Table III we show the angular correlation between kaons and pions, protons and pions, and between pions and pions with and without the presence of the resonances. When we remove the events with N^{*++} and K^{*0} , we see in Figs. 7(a), 7(b), and 7(c) that the angular correlation between $\pi^+\pi^+$, $\pi^-\pi^-$, and $\pi^+\pi^-$ becomes more isotropic. Thus we find that the resonances have a very dominating effect upon the angular correlations and after the removal of these resonances, the values of γ^L and γ^U for pions are very close to one another within the statistical uncertainties. It has been mentioned that the smaller angles between two particles of identical charges ($\pi^+\pi^+$, $\pi^-\pi^-$) are connected by the fact that the system is exotic. It has been further pointed out that a similar effect exists for $K\pi$ pairs, i.e., the average angle was less for $K^+\pi^+$ (i.e., exotic pairs) than for $K^+\pi^-$ or $K^0\pi^+$ (i.e., nonexotic pairs). But DeBaere *et al.*¹⁸ have observed no difference in γ for $K^+\pi^+$ and $K^+\pi^-$ pairs. We also disagree with the previous results²⁰ for correlation in kaon and pion angles.

3. Momentum Distributions

(a) *c.m. momentum distributions.* In order to see how effective the C \bar{L} A and the modified C \bar{L} A models are in reproducing the data correctly, we show in Fig. 8 the c.m. momentum distributions of the leading (K^+) and the target (p) particles. The modified C \bar{L} A model is found to fit the experimental data better than the C \bar{L} A model.

(b) *Transverse momentum distributions.* From the cosmic-ray data we have learned the presence of the leading particle, the small inelasticity of the collision and the smallness of p_t for many multiparticle production processes. The average p_t of the proton, kaon, and pions are shown in Table IV. The $\langle p_t \rangle$ increases slightly with the increase of mass of the particle. The transverse momentum distributions of K^+ , p , π^- , π^+ are

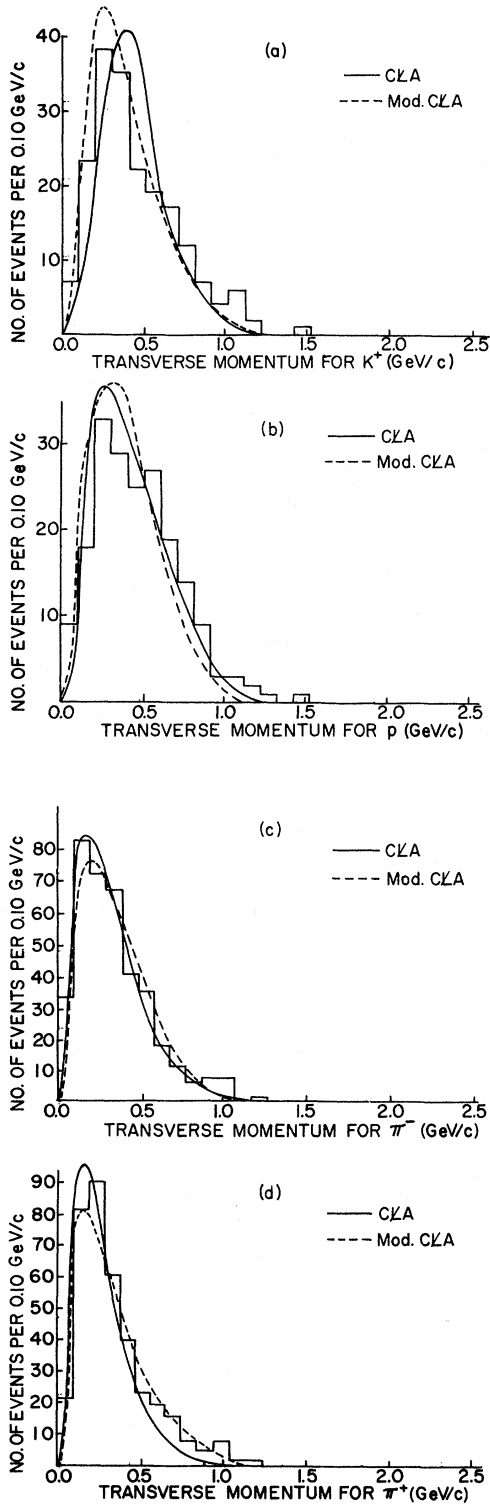


FIG. 9. Transverse momentum distributions for (a) K^+ , (b) p , (c) π^- , and (d) π^+ . The histograms display the experimental data and the smooth curves the theoretical predictions of (—) the CLA model and (---) the modified CLA model.

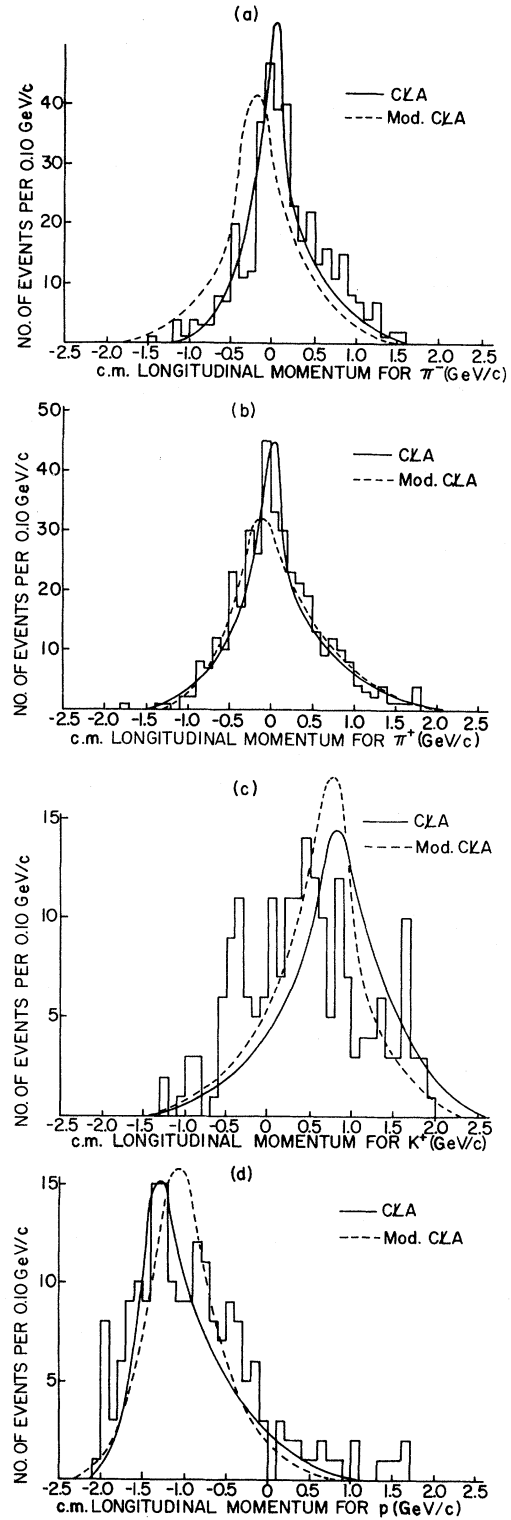


FIG. 10. Longitudinal momentum of (a) π^- , (b) π^+ , (c) K^+ , and (d) p in c.m. system. The histograms display the experimental data and the smooth curves the theoretical predictions of (—) the CLA model and (---) the modified CLA model.

shown in Figs. 9(a), 9(b), 9(c), and 9(d), respectively. The distributions of the pions are found to be very similar, while the proton and the kaon distributions exhibit a slightly broader structure. The theoretical curves due to the C \bar{L} A and the modified C \bar{L} A models reproduce the data fairly well.

(c) *c. m. longitudinal momentum distributions.*

One of the most sensitive variables to the reaction mechanism is the c.m. longitudinal momentum p_l^* . Longitudinal momenta are largely dependent on energy, multiplicity, and on the nature of the particle.

The c.m. longitudinal momentum distributions of π^- , π^+ , K^+ , and p are shown in Figs. 10(a), 10(b), 10(c), and 10(d), respectively. These distributions are compared with the predictions of the C \bar{L} A model (solid line) as well as with the modified C \bar{L} A model (dashed line). We see that the modified C \bar{L} A model represents a better fit to the data for K^+ , p , and π^+ , whereas the C \bar{L} A model is better for the π^- . The average c.m. longitudinal momentum of the π^- is found to be considerably greater than zero, as shown in Table IV. The absolute values of the longitudinal momenta of all the particles are also given in the same table. There is an interesting correlation between the momenta of the particles and the resonance production. The effect of $N^{*+}(1238)$ removal on the longitudinal momentum distribution of the positive pions is to remove pions from the backward hemisphere. This, of course, is expected, since we observe a similar effect in the angular distribution of the π^+ in the c.m. system. Similar results are obtained for the removal of $K^{*0}(890)$ events from the p_l^* plot of the negative pions, where we observe the reduction in the number of scattered pions of negative charges in the forward hemisphere. The predictions of the C \bar{L} A and the modified C \bar{L} A models are in agreement with the experimental data. One also finds a correlation between the longitudinal momentum of the proton and the leading kaon. In general, one can see that a large negative value of x (where $x = p_l^*/p_{l\max}$) for the protons corresponds to a small positive value of x for the K^+ , and that a large positive value of x for the K^+ corresponds to a small negative value of x for the proton.

4. Invariant-Mass Distributions

The only resonances which appear to occur in a measurable amount are the baryon resonance $N^{*+}(1238)$ and the strange mesonic resonance $K^{*0}(890)$. The partial cross sections are given in Table V. The other resonant states such as $Q^+(1300)$, $N^{*0}(1238)$, and $\rho^0(765)$ are observed,

TABLE V. Cross sections.

Reaction	Cross section (mb)
$K^+p \rightarrow 6$ charged prongs + neutrals	2.260 ± 0.054
$K^+p \rightarrow K^+\pi^+\pi^-\pi^+\pi^-p$ (final state)	0.251 ± 0.018
$K^+p \rightarrow K^{*0}(890)\pi^+\pi^-\pi^+p$	0.043 ± 0.007
$K^+p \rightarrow K^+\pi^-\pi^+\pi^-N^{*+}(1238)$	0.040 ± 0.009
$K^+p \rightarrow K^{*0}(890)\pi^+\pi^-N^{*+}(1238)$	0.041 ± 0.011

but only in small percentages. Figure 11 shows the invariant-mass distributions for different possible particle combinations. They show a significant deviation from the predictions of a pure Lorentz-invariant phase space. Apart from the expected deviations due to resonance productions of the $N^{*+}(\pi^+p)(1238)$, and $N^{*0}(p\pi^-)(1238)$, the mass distribution for three or more particles also shows deviations at both the low and high effective mass regions. In contrast, the kaon-pion(s) distribution(s) exhibit enhancement only in the low-effective-mass regions. The pion-pion(s) invariant-mass distribution(s) exhibit behavior similar to the kaon-pion(s) by deviating from the phase space only at low effective masses. The pK^+ and pK^+ + pion plots exhibit deviations at high effective mass. It is obvious from these distributions that the pions do not receive a major portion of the energy (pionization), while the proton in particular does retain a large fraction. The pions appear to scatter along the direction of the "leading" particles resulting in a high- or low-effective-mass enhancement. The C \bar{L} A and the modified C \bar{L} A models have been used to estimate the background in the various distributions. Using the background of the models is considered to be an improvement over phase space. Both the models however reproduce the general features of the data, i.e., the regions where deviations from phase space occur are predicted by both models. The modified C \bar{L} A model, on the average, predicts distributions which have smaller deviations from phase space than the C \bar{L} A model. The data also indicate this characteristic.

The deviations from Lorentz-invariant phase space appear to be adequately reproduced by the models for most cases, indicating that the dynamics of Reggeon exchange and the kinematics associated with the postulated low-invariant-mass clusters provide a reasonable and useful description for multiparticle production reactions.

B. Quark System

Recently, a Wisconsin group²¹ has found that the produced pions in 25-GeV/c π^-p inclusive reactions show a forward-backward asymmetry in the

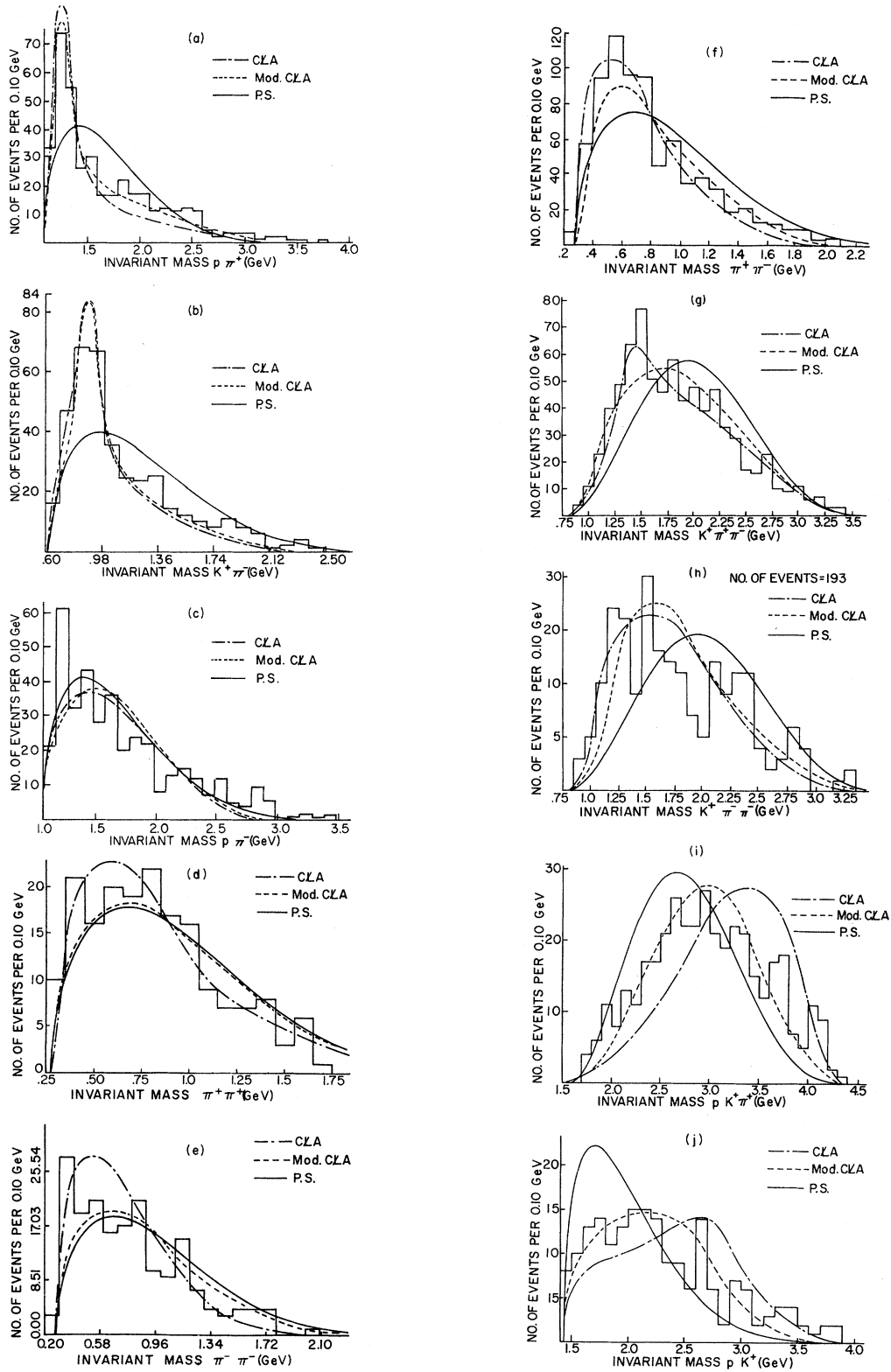


FIG. 11. Effective mass distributions of (a) $p\pi^+$, (b) $K^+\pi^-$, (c) $p\pi^-$, (d) $\pi^+\pi^+$, (e) $\pi^-\pi^-$, (f) $\pi^+\pi^-$, (g) $K^+\pi^+\pi^-$, (h) $K^+\pi^-\pi^-$, (i) $pK^+\pi^+$, and (j) $pK^+\pi^-$. The histograms display the experimental data, and the smooth curves the theoretical predictions of (---) the CLA model, (-·-) the modified CLA model, and (—) phase space.

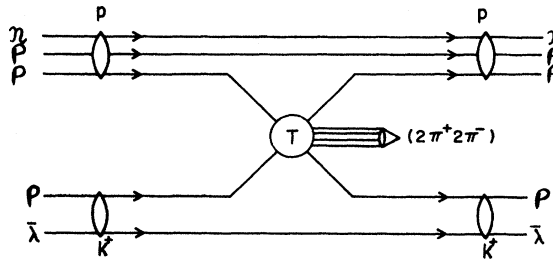


FIG. 12. Multipion production in quark-quark collisions for K^+p interaction.

center-of-mass longitudinal-momentum distribution. In order to distinguish the produced particles from the leading pions, the authors plotted forward emitted π^+ and backward emitted π^- mesons. They found asymmetry in the longitudinal-momentum distribution of the pions in the c.m. system. Defining the new coordinate system in terms of $R = p_p/p_\pi$, the ratio of incident proton to incident pion momenta ($R=1$ for c.m. system and $R=0$ in the laboratory frame), the symmetry can be obtained in the so-called Q (quark) system for which R equals 1.5. The authors point out that the ratio 3:2 is highly suggestive because of its implications for hadronic structure as postulated by the triplet quark model, and this was previously sug-

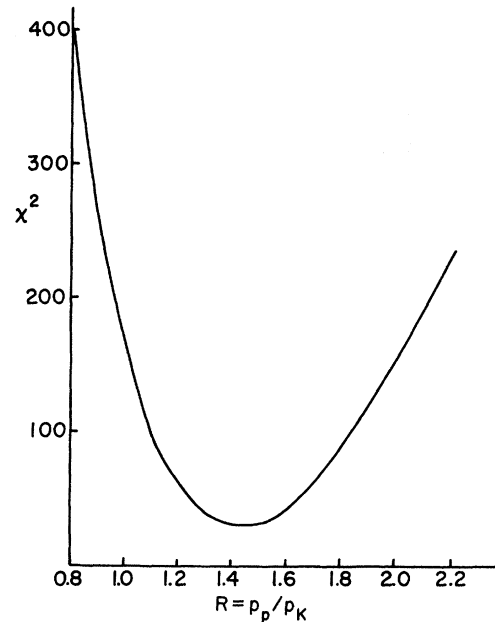


FIG. 13. χ^2 vs R for π^- particles produced in K^+p interactions.

gested by Satz³ in a somewhat similar context. This is shown in Fig. 12. We adopted the same procedure as followed by Elbert *et al.*²¹ in finding

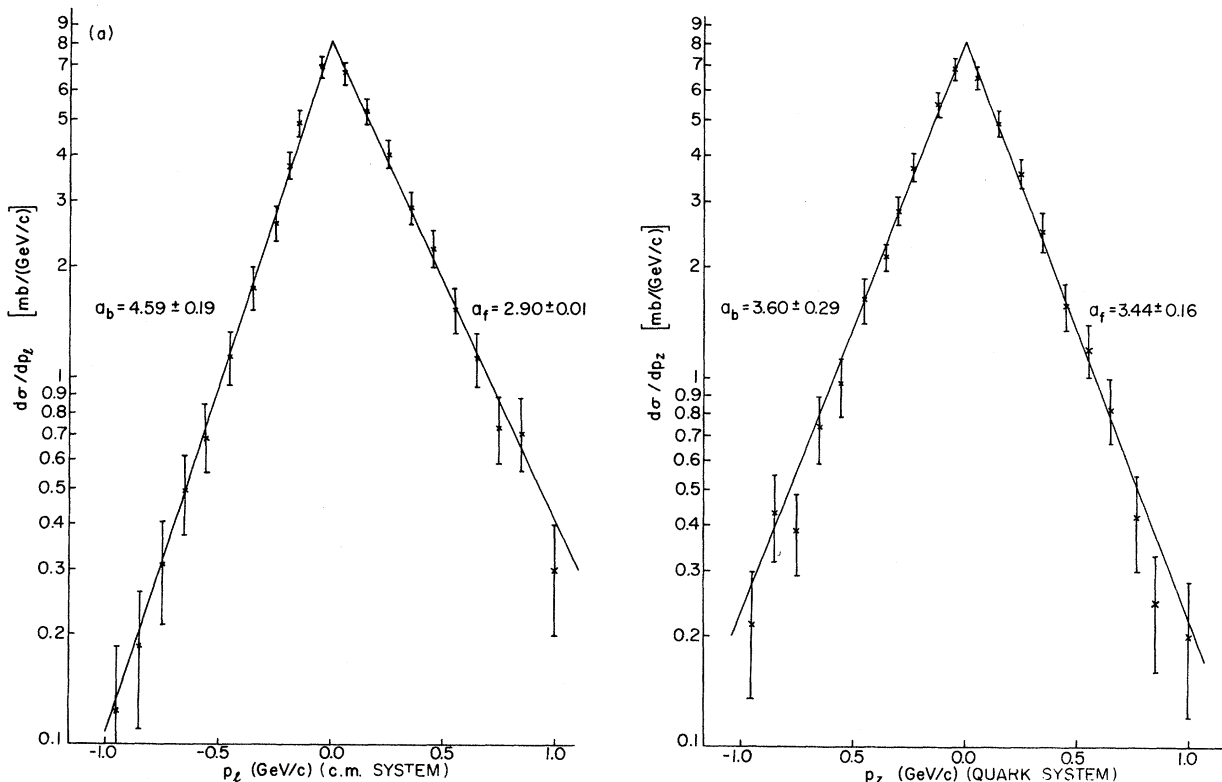


FIG. 14. Longitudinal momentum distributions of π^- mesons in K^+p interactions (a) in the c.m. system ($R=1$) and (b) in the quark frame ($R=1.5$).

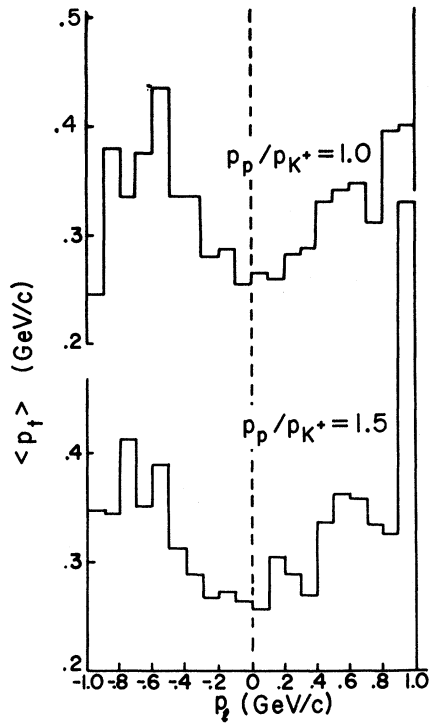


FIG. 15. Plots of the average transverse momentum $\langle p_t \rangle$ for negative produced pions as a function of longitudinal momentum p_l . (a) in the c.m. system ($R=1.0$) and (b) in the quark frame ($R=1.5$).

Lorentz frames in which the longitudinal momentum (p_z) distribution is centered about zero and is symmetric. For K^+p reactions, the negative pion can be easily identified without constraining it to either the forward or backward hemisphere. Using the nearly 3500 negative pions produced in the 6-prong K^+p reaction at 12.7 GeV/c, we have attempted to symmetrize the longitudinal momen-

tum p_z . Figure 13 shows the χ^2 for various ratios of proton to K^+ momenta used in the Lorentz transformation. The χ^2 was defined by

$$\chi^2 = \sum_i \frac{(\sigma_F^i - \sigma_B^i)^2}{(\delta_F)_i^2 + (\delta_B)_i^2}, \quad (3)$$

where σ_F^i (σ_B^i) is the cross section for the i th bin in the forward (backward) p_z distribution, and $(\delta_F)_i$ is the associated error. The minimum for the χ^2 was found to occur for $R=1.5$. For this value of the ratio the greatest symmetry occurs. For 6-prong events in π^+p interactions at 7 GeV/c, Stone *et al.*²² also found that $R \sim 1.5$ produced the best symmetry for the longitudinal momentum distribution. It appears that for quite different beam particles and energies and for the same multiplicity, the value $R=1.5$ is obtained. The symmetry in the longitudinal momentum distribution is further compared by the slopes obtained for exponential fits to the backward and forward hemisphere of the longitudinal momentum distribution in the c.m. system ($R=1.0$) and in the "quark" frame ($R=1.5$). The results were fitted with an exponential function, i.e., $Ae^{-a_i p_l}$, where $a_i = a_F$ (forward), a_B (backward). For c.m. system ($R=1.0$) and for quark frames ($R=1.5$) the results are shown in Figs. 14(a) and 14(b), respectively. The results are summarized in Table I.

Since the distribution of transverse momenta for secondary particles (p_t) is independent of their longitudinal momenta (p_l), the primary energy of the particle, and the kind of primary hadron, it is worth mentioning that there is some indication of a quark system in the behavior of p_t . The effect is not as pronounced as the one exhibited by p_l alone, but it is nevertheless significant. This is illustrated in Fig. 15, where the $\langle p_t \rangle$ is plotted as a function of the longitudinal momentum p_l for the

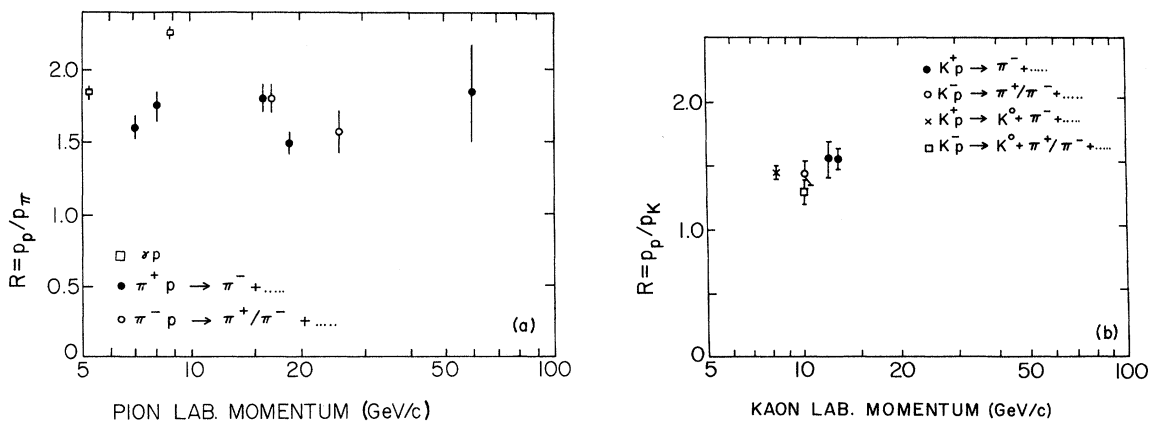


FIG. 16. R values found as a function of laboratory momentum in (a) π^+p interaction, (b) K^+p interactions. The non-overlapping errors of some experiments at nearby incident momenta are probably due to different ranges of p_l used in fitting exponentials to the p_l distributions. Part (a) also has points for the γp interaction.

entire sample of negative pions. A tendency is indicated toward greater forward-backward symmetry as R varies from 1.0 to 1.5. The distributions exhibit the characteristic dip at $p_t = 0$ and show some indication of a quark system behavior in $\langle p_t \rangle$ also.

This result was interpreted as evidence in favor of the quark model. Similar asymmetry was observed by Ko and Lander²³ at 12 GeV/c in $K^+p \rightarrow \pi^- + \text{anything}$. Figures 16(a) and 16(b) give²⁴ all the R values which were required to produce symmetry in the p_t distributions of π^+p and K^+p interactions, respectively. It appears that there is no tendency for R to become smaller or larger with increasing energy. The scaling prediction²⁵ that R should be approximately energy-independent is certainly not strongly violated. One may notice, however, a slight difference in the value of R for experiments with incoming kaons and pions, indicating perhaps a dependence of the parameter R on the mass of incoming particle. The value of R , equal to 1.0 for pp collisions, increases with the decreasing mass of the projectile and is approximately 1.5 for K^-p , 1.75 for πp , and 2.0 or larger for γp collisions.²⁶

Apart from the p_t and p_t distributions, we also looked at the angular distribution between the scattered π^- and incident K^+ which is plotted in Fig. 17. The histograms in solid and in dashed lines indicate the angular distributions in the c.m. ($R=1.0$) and the quark ($R=1.5$) systems, respectively. For the quark frame, the distribution is fairly symmetric about $\theta = \pi/2$.

A serious objection to the attractive idea of multiparticle production by quark-quark collision

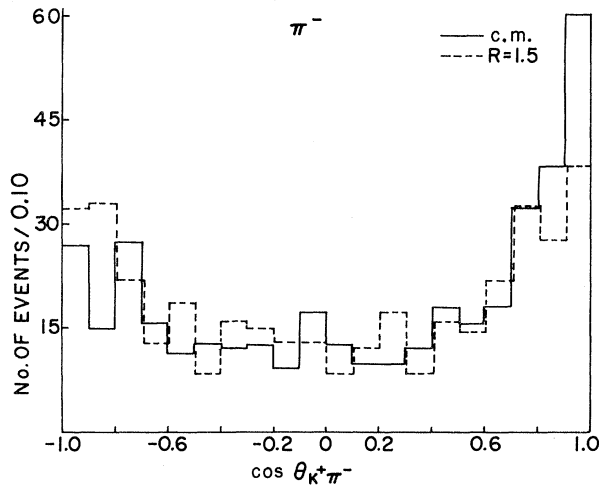


FIG. 17. Angular distributions for all π^- produced in the c.m. system ($R=1.0$) and in the quark frame ($R=1.5$) for K^+p interaction.

comes from a fact already noticed by the Wisconsin group.²¹ R strongly depends on the number of particles produced in the interaction. The values of the parameter R decrease strongly with increasing multiplicity. This dependence is well established²⁵ and can be explained on the basis of double-quark scattering for high multiplicities. We may, however, mention that Caneschi²⁷ and Friedman and Risk²⁸ have shown that the dependence of R on the multiplicity can be explained by multiperipheral models.

C. Rapidity Distribution

Another possible way of finding asymmetry in meson-proton interactions is to look at rapidity distributions of the produced pions. Rapidity Y is defined as

$$\begin{aligned} Y &= \frac{1}{2} \ln[(E + p_t)/(E - p_t)] \\ &= \sinh^{-1}[p_t/(m^2 + p_t^2)^{1/2}] \\ &= \cosh^{-1}[E/(m^2 + p_t^2)] . \end{aligned} \quad (4)$$

The shape and magnitude of rapidity distributions are invariant with respect to Lorentz transformations along the incoming particle direction, i.e.,

$$y_{(1)} = y_{(2)} + \frac{1}{2} \ln[(1 + \beta)/(1 - \beta)] , \quad (5)$$

where β is the velocity of system (1) with respect to system (2). We may also point out that if there is a symmetry system which is moving along the incident particle direction, the longitudinal rapidity distribution should be symmetric with respect to given Y_s , the rapidity of the symmetry system. The displacement of the central value of Y_s from $Y=0$ is directly related to the parameter R_s by Y_s

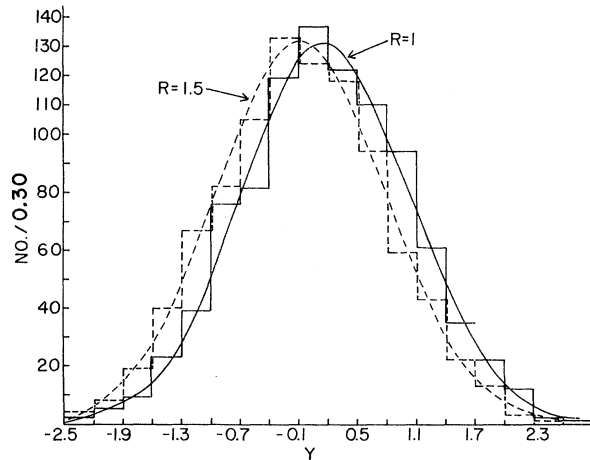


FIG. 18. Rapidity distribution for π^- meson in (a) the c.m. system $R=1$ and (b) the quark system $R=1.5$. The histograms display the experimental data, and the smooth curves are the Gaussian curves fitting the data.

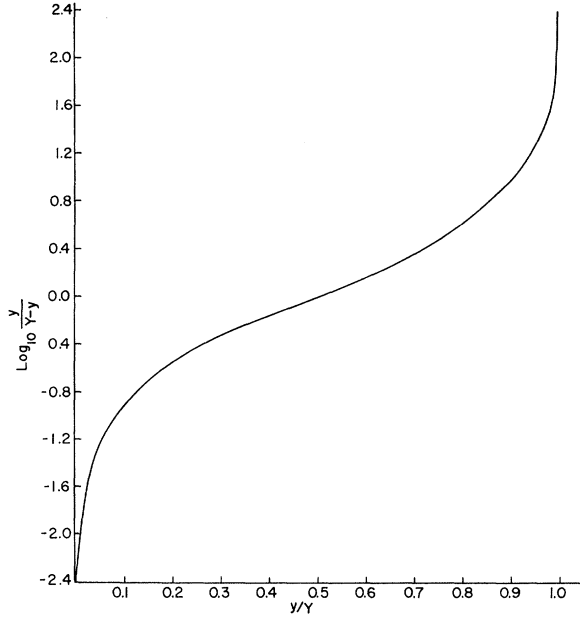


FIG. 19. The Duller-Walker plot for the π^- , i.e., $\log_{10}[F/(1-F)]$ vs y/Y (the rapidity y is linearly related to $\log_{10} \tan \theta_t$).

$\approx \frac{1}{2} \ln R_s$. If the symmetry system exists, R_s should be identical to R , where $R = P_p^{inc}/P_\pi^{inc} = 1.5$. In Fig. 18 we show the rapidity distribution for π^- in the c.m. system ($R=1$) and the quark system ($R=1.5$). The Y distribution is approximately Gaussian and symmetric in both cases with center of symmetry at $Y_{c.m.}^0 = 0.17$ and $Y_q^0 = -0.10$. The slope in either case is about 1.1 ± 0.15 .

D. Two-Fireball Model

In order to see if there is any partial evidence for the two-fireball model, we have plotted in Fig. 19 the forward/backward fraction $F/(1-F)$, which is simply $[y/(Y-y)]$, against y/Y , where Y is the maximum value of rapidity²¹ and y is linearly related to $\log_{10} \tan \theta_t$. The resulting Duller and Walker plot²⁹ is shown in Fig. 19. We see no indication of the two fireballs at this energy.

E. Transverse Momentum Distributions

It has been a common practice to fit the p_t distributions with theoretical curves. In Fig. 20 we show two distributions, i.e. (i) the Hagedorn distribution [$N \sim H_1 p_t^{3/2} \exp(-p_t/H_2)$], and (ii) the Boltzmann distribution [$N \sim B_1 p_t \exp(-p_t^2/B_2)$], where $H_2 = 0.12 \pm 0.002$ and $B_2 = 0.09 \pm 0.004$. One can see that the Hagedorn distribution gives the best fit to the data, giving the most probable value of the transverse momentum to be 200 MeV/c. Our results are compared with other data³⁰ in Ta-

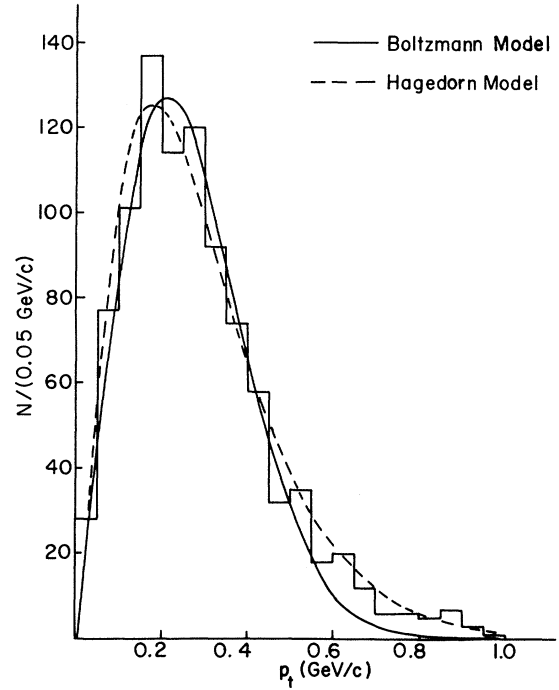


FIG. 20. p_t distribution for negative pions. The histogram displays the experimental data, and the smooth curves the theoretical predictions due to (—) the Boltzmann distribution ($N \sim B_1 p_t \exp(-p_t^2/B_2)$) and (---) the Hagedorn distribution ($N \sim H_1 p_t^{3/2} \exp(-p_t/H_2)$).

ble VI. The average value of the transverse momentum of the π^- was found to be 350 MeV/c, in agreement with other observations made from bubble-chamber data in which the projectiles were different.

Valuable information about inclusive reactions can also be obtained from the study of transverse momentum distributions. In Fig. 21 are shown the p_t^2 distributions of π^- from 6-prong $K^+ p$ interactions at 12.7 GeV/c. Assuming $d\sigma/dp_t^2 = a \exp(-bp_t^2)$, the value of the slope (b) is found to be 11.8 ± 0.06 (GeV/c)⁻². The slope for pions produced in pp in-

TABLE VI. Comparison of Boltzmann ($N \sim p_t \exp(-p_t^2/B_2)$) and Hagedorn ($N \sim p_t^{3/2} \exp(-p_t/H_2)$) constants (B_2, H_2) for pions in different reactions.

Interaction	Boltzmann constant (B_2)		Hagedorn constant (H_2)	
	π^-	π^+	π^-	π^+
$K^+ p$ 12.7 GeV/c	0.09 ± 0.004		0.12 ± 0.002	
$\pi^- p$ 25 GeV/c		0.149		0.131 ± 0.036
pp 28.5 GeV/c	0.129		0.127 ± 0.036	
pp 13 GeV/c	0.126		0.126 ± 0.039	
$p\bar{p}$ 2.32 GeV/c		0.132		0.129 ± 0.011
$p\bar{p}$ 5.7 GeV/c	0.149	0.149	0.137 ± 0.022	0.137 ± 0.022

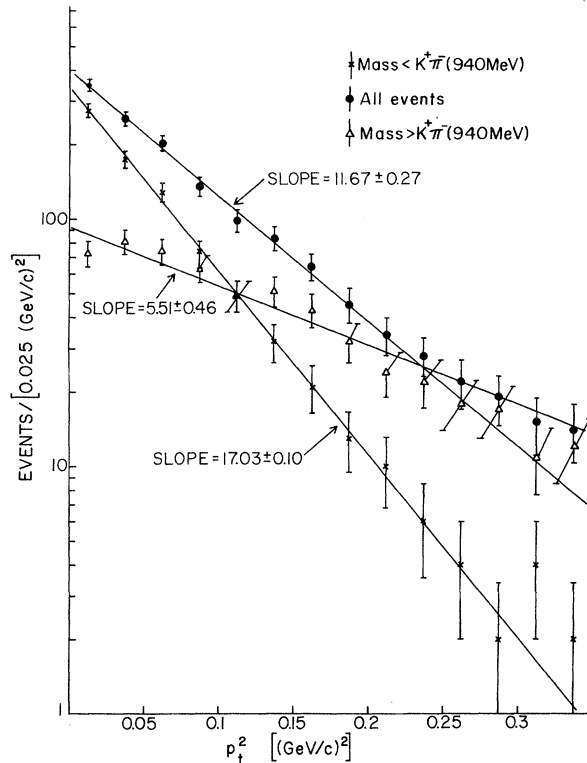


FIG. 21. p_t^2 distribution for π^- mesons in K^+p interactions. (i) All events, (ii) events with invariant-mass $M(K^+\pi^-) < 940$ MeV; (iii) invariant-mass $M(K^+\pi^-) > 940$ MeV.

interactions at 6 GeV/c (Ref. 31) was found to be 8.78 ± 0.51 [for $p_t^2 < 0.2$ (GeV/c) 2]. In Fig. 21 is also shown the distribution of p_t^2 for π^- meson when events having an invariant-mass $M(K^+\pi^-)$ are either selected or excluded. The steep maximum at small p_t^2 is clearly related to low $M(K^+\pi^-)$ events. The slope values for events with $M(K^+\pi^-) < 940$ MeV and > 940 MeV are 17.03 ± 0.10 and 5.51 ± 0.46 , respectively. Similarly for π^-p interaction at 16 GeV/c, it was found³² that the slopes of p_t^2 distributions for events having invariant-mass $M(p\pi^+) < 1.36$ GeV and > 1.36 GeV are $b = 20.7$ and 7.67 ,

respectively. The presence of resonances do affect the slope of the p_t^2 distributions.

V. CONCLUSION

We have analyzed events of the type $K^+p \rightarrow K^+p2\pi^+2\pi^-$ interactions at 12.7 GeV/c which are highly peripheral with significant resonance production. The CZA model, in which the multiperipheral mechanism with exchange of Regge trajectories is assumed, gave a good description of the data. An improvement of the CZA model was achieved by replacing t by $t - t_{\min}$ in the calculation of the amplitudes for the multiperipheral diagrams.

The GGLP effect, observed in the opening angle of the distributions of pairs of pions, is seen but disappears after the removal of resonances.

The search for a frame of reference suggested by the quark model resulted in a symmetric longitudinal momentum distribution for the negative pions in this reaction when the ratio of the momenta of the proton and K^+ was approximately $\frac{3}{2}$. Quark-system behavior was noted for the angular distributions and the average transverse momentum as a function of longitudinal momentum. Single-particle inclusive distributions have been presented for comparison with other experiments. We find a correlation between low values of p_t and p_t which may be partially due to peripheral resonance production in these data. The rapidity distributions for π^- meson in the c.m. system ($Y_{c.m.}$) and in quark system (Y_q) are presented. The p_t momentum distribution for negative pions is best fitted by Hagedorn's distribution. The slope for the p_t^2 distribution for negative pions is comparable with other data, and we do not see any indication of two fireballs in K^+p interaction at 12.7 GeV/c.

ACKNOWLEDGMENT

We are very grateful to Professor T. Ferbel for the use of the bubble-chamber film from which we obtained our data in the present analysis.

¹A. Białas and T. Ruijgrok, Nuovo Cimento **39**, 1061 (1965).

²R. Hagedorn, Nuovo Cimento Suppl. **3**, 147 (1965); CERN Reports No. TH 51, No. TH 827, No. TH 853, and No. TH 851.

³H. Satz, Phys. Lett. **25B**, 27 (1967); Phys. Lett. **25B**, 220 (1967); Phys. Rev. Lett. **19**, 1453 (1967); and J. J. Kokkedee and L. Van Hove, Nucl. Phys. **B1**, 169 (1967).

⁴K. A. Ter-Martirosyan, Zh. Eksp. Teor. Fiz. **44**, 341 (1963) [Sov. Phys.-JETP **17**, 233 (1963)]; Nucl. Phys.

68, 591 (1965); T. W. B. Kibble, Phys. Rev. **131**, 2282 (1963).

⁵Chan Hong-Mo, K. Kajantie, and G. Ranft, Nuovo Cimento **49**, 157 (1967).

⁶Chan Hong-Mo, J. Loskiewicz, and W. W. M. Allison, Nuovo Cimento **57A**, 93 (1968).

⁷M. Bardadin-Otwinowska *et al.*, Phys. Rev. **4**, 2711 (1971).

⁸W. M. Labuda, Ph.D. thesis, SUNY at Buffalo, 1971 (unpublished).

⁹O. Czyżewski, in *Proceedings of the International Conference in*

- High Energy Physics, Vienna, 1968*, edited by J. Prentki and J. Steinberger (CERN, Geneva, 1968).
- ¹⁰S. O. Holmgren, S. Nilsson, T. Olhede, and N. Yamdagni, *Nuovo Cimento* **57A**, 20 (1968).
- ¹¹G. Goldhaber, W. B. Fowler, S. Goldhaber, T. F. Hoang, T. E. Kalogeropoulos, W. M. Powell, *Phys. Rev. Lett.* **3**, 181 (1959); G. Goldhaber, S. Goldhaber, W. Lee, and A. Pais, *Phys. Rev.* **120**, 300 (1960).
- ¹²Aachen, Berlin, Bonn, Hamburg, München Collaboration, *Nuovo Cimento* **42A**, 954 (1966).
- ¹³Bonn, Durham, Nijmegen, Paris (E.P.), Turin Collaboration, *Phys. Rev.* **161**, 1356 (1967).
- ¹⁴J. Bartke, O. Czyżewski, J. A. Danysz, A. Eskreys, J. Łoskiewicz, P. Malecki, J. Zaorska, K. Eskreys, K. Juszczak, D. Kisielewska, W. Zielinski, M. Szeptycka, K. Zalewski, G. Pichon, and M. Rumpf, *Phys. Lett.* **24B**, 163 (1967); M. Bardadin-Otwinowska, M. Danysz, T. Hofmoki, S. Otwinowski, H. Piotrowska, R. Sosnowski, M. Szeptycka, A. Wroblewski, Institute of Nuclear Research, Warsaw Report INR NO. 761/VI/PH, 1966 (unpublished).
- ¹⁵P. Daronian, A. Daudin, B. Gandois, C. Kochowski, L. Mosea, CERN Report No. 68-7, Vol. 2, 1968 (unpublished).
- ¹⁶K. Bockmann, H. Drevermann, K. Sternberger, N. Stief, T. Hofmoki, L. Michejda, S. Otwinowski, H. Piotrowska, R. Sosnowski, M. Szeptycka, W. Wojeik, and A. Wroblewski, Institute of Nuclear Research, Warsaw Report "P" No. 837/VI/PH, 1967 (unpublished).
- ¹⁷S. O. Holmgren, S. Nilsson, T. Olhede, and N. Yamdagni, *Nuovo Cimento* **57**, 20 (1968).
- ¹⁸W. DeBaere, J. Debaisieux, E. DeWolf, P. Dufour, F. Gard, P. Herquet, J. Heughebaert, L. Pape, P. Peters, F. Verbeure, G. Charriere, D. Drigard, W. M. Dunwoodie, A. Eskreys, Y. Goldschmidt-Clermont, A. Grant, V. P. Henri, F. Muller, Z. Šékera, and J. K. Tuominiemi, *Nucl. Phys.* **B22**, 131 (1970).
- ¹⁹O. Czyżewski and M. Szeptycka, *Phys. Lett.* **25B**, 482 (1967).
- ²⁰Bruxelles-CERN-Cracow Collaboration, A. Eskreys *et al.*, *Nucl. Phys.* (to be published).
- ²¹J. W. Elbert, A. R. Erwin, and W. D. Walker, *Phys. Rev. D* **3**, 2043 (1971).
- ²²S. L. Stone, D. Cohen, M. Farber, T. Ferbel, R. Holmes, P. Slattery, and B. Werner, *Nucl. Phys.* **B32**, 19 (1971).
- ²³J. Ko and R. L. Lander, *Phys. Rev. Lett.* **26**, 1064 (1971).
- ²⁴O. Czyżewski, in *Proceedings of the Colloquium on Multiparticle Dynamics, University of Helsinki, 1971*, edited by E. Byckling, K. Kajantie, H. Satz, and J. Tuominiemi (Univ. of Helsinki Press, Helsinki, 1971).
- ²⁵C. E. DeTar, *Phys. Rev. D* **3**, 128 (1971).
- ²⁶K. C. Moffeit *et al.*, *Phys. Rev. D* **5**, 1603 (1972).
- ²⁷L. Caneschi, *Phys. Rev. D* **3**, 2865 (1971).
- ²⁸J. H. Friedman and C. Risk, *Phys. Rev. D* **5**, 2245 (1972).
- ²⁹M. Duller and W. D. Walker, *Phys. Rev.* **93**, 215 (1954); G. Cocconi, *Phys. Rev.* **111**, 1697 (1958).
- ³⁰T. F. Hoang, *Nucl. Phys.* **B38**, 333 (1972).
- ³¹M. A. Abolins *et al.*, *Phys. Rev. Lett.* **25**, 126 (1970).
- ³²Aachen-Berlin-Bonn-CERN-Cracow-Heidelberg-Warsaw-Collaboration, in *Proceedings of the Amsterdam International Conference on Elementary Particles, 1971*, edited by A. G. Tenner and M. Veltman (North-Holland, Amsterdam, 1972).

Large-Angle Quasielastic Electron-Deuteron Scattering*

K. M. Hanson,[†] J. R. Dunning, Jr.,[‡] M. Goitein,[§] T. Kirk,^{||} L. E. Price,^{**} and Richard Wilson

Harvard University, Cambridge, Massachusetts 02138

(Received 28 September 1972)

Measurements of differential cross sections for quasielastic electron-deuteron scattering $e + d \rightarrow e + p + n$ have been made in which recoil protons were detected in coincidence with the scattered electrons. The ratios of the elastic electron-neutron to the electron-proton scattering cross sections are derived from the proton coincidence data. For comparison, these ratios are also determined from the scattered-electron momentum spectra using the peak and area methods. The theory developed by Renard, Tran Thanh Van, and LeBellac, which includes corrections for the final-state interactions, is found to explain the proton coincidence results. The present measurements, made at an electron scattering angle of 90° for four-momentum transfers of $q^2 = 7, 10, 15,$ and 29 F^{-2} , and at 80° for $q^2 = 45 \text{ F}^{-2}$, are combined with previous results to obtain the electromagnetic form factors of the neutron.

I. INTRODUCTION

The quasielastic electron-deuteron process $e + d \rightarrow e + n + p$ has been investigated. The aim of the measurements presented here is to provide information about the electric and magnetic form factors of the neutron, G_{En} and G_{Mn} . The present experiment extends the proton coincidence method

used by Budnitz *et al.*¹ to large electron-scattering angles.

In the proton coincidence method, protons which recoil in the direction of momentum transfer are detected in coincidence with scattered electrons. Quasielastically scattered electrons which possess protons in coincidence, "ep events," arise mainly from the interaction of the electron with the proton